A Versatile Method for Coating Surfaces with Functional and Responsive Polymer-Based Films

Qiang Matthew Zhang,[a] Michael J. Serpe*[a]

[a] Department of Chemistry, University of Alberta, Edmonton, AB, Canada, T6G 2G2
11227 Saskatchewan Drive E-mail: michael.serpe@ualberta.ca

KEYWORDS: Surface modification; Responsive microgels; Responsive polymers; Functional Coatings; Sensing

ABSTRACT: A versatile surface modification technique was developed to yield poly (N-isopropylacrylamide) (pNIPAm) microgel-based thin films on a variety of substrates, e.g., metals, non-metals, and polymers. Since the chemistry, and hence functionality and responsivity, of the pNIPAm-based microgels is easily tuned, multifunctional and responsive thin films could be generated on many different surfaces without varying the coating conditions. In one case, we showed that fluorescent/light emitting thin films could be generated using crystal violet-modified microgels. Antibacterial films could be obtained using silver nanoparticle-modified pNIPAm-based microgels. Finally, we show that thin films fabricated via the methods here could be used as a component in optical sensors. While we show only a few examples of the utility of this approach, we feel that the apparent universality of the technique can be extended to countless other applications.

1. INTRODUCTION

A variety of devices and machinery used in our everyday lives have components that interact with one another, e.g., automobile engines, door hinges, and bone joints in our bodies. Oftentimes, the lifetime and utility of these devices and machinery depends on the mechanical properties of materials, and how they interact chemically with each other and their environment. Their interactions rely on many factors -- e.g., surface roughness and porosity, although much can be attributed to the chemistry of the material's surfaces and interfaces.[1-3] In order to control these chemical interactions, organic molecule-modified surfaces have become very important for improving materials properties or even endowing materials with new properties.[4, 5] For example, functionalization of surfaces to render them antimicrobial is extremely important for sterilization of equipment and implants commonly used in the health sector.[6-8]

Many approaches for depositing coatings and films on material surfaces exist, and a few have emerged as the most common; for example, self-assembled monolayers (SAMs);[9-11] layer-by-layer self-assembly;[12] spin coating;[13] and surface polymerizations[14]. The most common example of a SAM is thiol self-assembly on Au-coated surfaces.[15-17] Thiol-based SAMs have been used to generate nanopatterns,[18, 19] molecular-scale devices,[20] optical materials,[21] biologically active surfaces[22] and as supports for cell culture.[23] While thiol-based SAMs are incredibly important, they do suffer from instabilities when exposed to certain environments, which can lead to film degradation. [24, 25] For example, degradation and contamination has been observed after as little as 1–2 weeks at room temperature in air,[24] and 70% of SAM layers are lost by simple immersion in pure THF at room temperature for 24 hours.[25] Layer-by-layer assembled thin film surface coatings have been shown to be more stable than thiol-based SAMs, but they also exhibit specific disadvantages. For example, polymer-based layer-by-layer assembled thin films assembled by electrostatic interactions have been shown to degrade significantly when exposed to solutions of that interfere with the layer-layer interactions, e.g., solution pH and ionic strength.[26] Furthermore, the layer components need to be chosen carefully such that the surface-polymer and polymer-polymer interactions yield film growth.[27] Spin coating-based approaches suffer from similar problems as the layer-by-layer assembled thin films, while surface polymerizations are complex and time consuming due to the fact that surfaces need to be premodified with reactive groups to participate in polymerization,[12, 28] among other things.[29]

Each surface modification approach listed above has certain pros and cons; common to all is the requisite strong affinity of the surface for the coating. To make surface modification simpler, and more efficient surface modification procedure capable of coating surfaces of various compositions, chemistry, and morphology is needed. Additionally, the ability to readily tune the chemical and physical properties of the film would be highly advantageous. Toward this end, mussel-inspired surface chemistry has been exploited.[30-34] Mussels have been shown to attach to many different types of inorganic and organic surfaces, including classically adhesion-resistant materials, e.g., poly(tetrafluoroethylene) (PTFE).[30] Mussels adhere to solid surfaces with mussel foot protein (mfps)-rich byssus as the holdfast. Catechol and its derivatives, which mimic the composition of mfps, can form surface-adherent films on virtually any material surface. [35] The coating process is achieved by catechol transformation into reactive quinones or semiquinones under oxidative conditions, subsequently forming strong irreversible covalent bonds on material surfaces, and giving rise to intermolecular crosslinking of polymers.[33, 36, 37] The Messersmith group developed various surface coatings based on polyphenols, which have been used as catalysts, antifouling materials, and tissue adhesives.[38-41] Israelachvili and Waite further investigated interactions of polyphenol and mfps with substrate surfaces, and many systems have been used as coating film and self-healing materials.[42-44] Subsequently, polyphenol-based coatings were further developed for: chiral recognition, [45] drug delivery, [46] lithium batteries, [47] nanofibers, [48] and mesoporous materials.[49] Several new catechol end capped polymers, composed of functional oligomers such as peptides [50] and poly(ethylene glycol),[51] were designed and reported for specific applications. The surface modification system, which allows for facile tenability and variation of surface functionality and responsivity, innovate the application of old materials.

The work here describes the generation of poly (N-isopropylacrylamide) (pNIPAm) hydrogel particle (microgel)-based thin films on a variety of substrates by exploiting polydopamine's ability to "universally" coat surfaces. PNIPAm-based microgels are highly porous, crosslinked

and water-soluble hydrogel particles with diameters on the order of 100's of nm to several micrometers. PNIPAm-based microgels are thermoresponsive, exhibiting a lower critical solution temperature (LCST) of 32 °C in aqueous environments. Therefore, above this temperature the pNIPAm-based microgels undergo a volume phase transition (VPT) from a water swollen to a deswollen/collapsed state.[52] The chemistry and functionality of pNIPAm-based microgels is very easily modified by copolymerization and/or post polymerization modification, which have allowed them to be made responsive to temperature and pH,[53] temperature,[54] and light.[55]

Here, we combine the versatile and easily tuned chemistry of pNIPAm-based microgels with polydopamine's ability to coat virtually any surface, to make functional and responsive polymer-based films on a wide variety of surfaces. Using this approach, we were able to readily generate coatings from fluorescent microgels, microgels modified with a two-photon-excited fluorophore (pyridinium hemicyanine), and Ag nanoparticle-modified microgels. Finally, a sensor device was fabricated from the resultant coatings. In each case, the surface coating retained the functionality, properties, and/or responsivity of the precursor microgels, which can be used for photonic materials, sensors, biomaterials and any endless other applications.

2. Results and discussion

2.1 Preparation of microgel films

Coatings were generated by immersing substrates into aqueous solutions (pH = 8.5) of dopamine and microgels. Under these conditions, dopamine's catechol group readily oxidizes to form the reactive quinone that can further undergo Michael-type addition or Schiff base formation with amine groups, and radical coupling with other catechols.[56] We hypothesized that if the polydopamine film formation proceeded in the presence of pNIPAm-based microgels, that they would be trapped and strongly adhered to the substrate of interest. The proposed mechanism is shown schematically in Figure 1a.

Figure 1. (a) Schematic of the proposed film structure; (b) light microscope image (scale bar is 4 µm); and (c,d) SEM images of MG-AAC-10% films generated on glass slides.

(a)

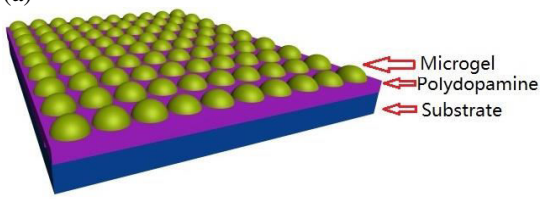

(b) (c)

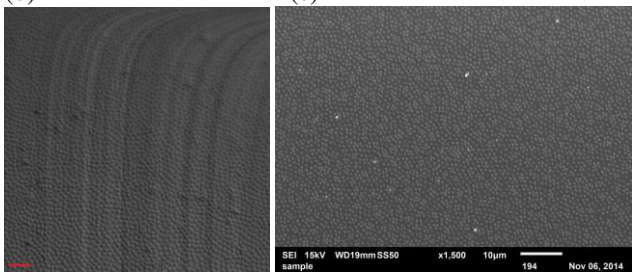

(d)

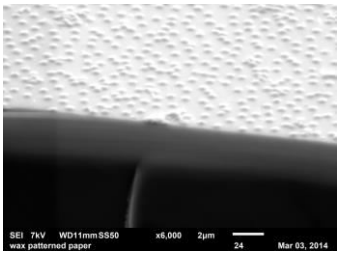

Our initial experiments focused on coating glass substrates with pNIPAm-co-acrylic acid microgels (MG-AAC); the microgels were composed of 10% AAC (mol AAC/total mol monomer and crosslinker), and denoted as MG-AAC-10%. The microgel synthesis is described in supporting information (SI). In order to optimize the film formation conditions, different mass ratios of microgels to dopamine were investigated. We found that a 5:100 mass ratio yielded surfaces coated uniformly with microgels. As can be seen in Figure 1, optical and scanning electron microscopy (SEM) images revealed that microgels were closely packed in the polydopamine films, as a single layer. Additionally, we measured the water contact angle of the resultant film, which was 40°. This is slightly higher than both the glass slide (32°), and the polydopamine-coated glass (35°). The results for other mass ratios are shown in Fig. S1.

Control experiments were also completed by exposing glass substrates to dopamine or microgels separately, and the results are shown in Figure S2. Dopamine films with small aggregates (features on the order of nanometers) formed on glass slides in the absence of microgels. Additionally, overnight exposure of the glass slides to a same concentration of microgels used to make the films in Figure 1 showed nearly no microgel adhesion after copiously rinsing with DI water (Figure S2c). Finally, in order to further investigate the film formation mechanism, substrates were exposed to dopamine only, and microgels added after 2 h and 5 h of dopamine polymerization. We observed that the number of microgels adhered to the substrates decreased as the dopamine polymerization time was increased prior to microgel addition (Figure S3). These data together support the hypothesis that the microgels must first adhere to the surfaces, followed by dopamine polymerization to fix the microgels on the surface.

We further demonstrated that this approach could be used to modify many different substrates using the same coating conditions as above, including metals (Al and Au), non-metals (Si and glass), and polymers (polytetrafluoroethene (PTFE), polystyrene (PS)). SEM images of the resultant microgel films are shown in Figure 2. As can be seen, the density of the microgels attached to the surface depended greatly on the substrate composition. To understand this phenomenon better, contact angles were measured for these materials before surface modification -- photographs of the water drops on each substrate are shown in Figure 2. We observed that the microgel surface coverage increased with increasing hydrophilicity of material's surface. Specifically, microgels were uniformly yet sparsely dispersed on PTFE surface (contact angle: 118°) (Figure 2a). When the substrate was relatively hydrophilic, e.g., glass (contact angle: 32°) and Al (contact angle: 25°), the surface coverage increased. Based on these results, we propose that hydrophilic surfaces can promote hydrophilic microgel adhesion, which

can then be trapped by dopamine polymerization, while this mechanism is not as prominent on the more hydrophobic surfaces. After modification by microgel films, the contact angles of PTFE and PS decreased by 20°, indicating that they become more hydrophilic. Upon incubating all these films in PBS buffer over a period of one week, both the morphologies and the contact angles were not significantly affected making them more stable than thiol-based SAMs and layer-by-layer assembled thin films.[24-26] As a control, all the substrates were exposed to microgels (same concentration as above) in the absence of dopamine. The images in Figure 2 (left insets) show that no microgels stick to the surfaces in the absence of dopamine. Almost no microgels were observed on these material surfaces, further indicating that microgels were entrapped by crosslinked polydopamine networks.

Figure 2. SEM images of microgel films formed on the different indicated substrates: (a) PTFE, (b) PS, (c) Al, (d) Au, (e) Si, and (f) Glass. **Right insets: photographs of a drop of water on the substrates before film formation. Left insets: substrates after treatment with microgels in absence of dopamine.**

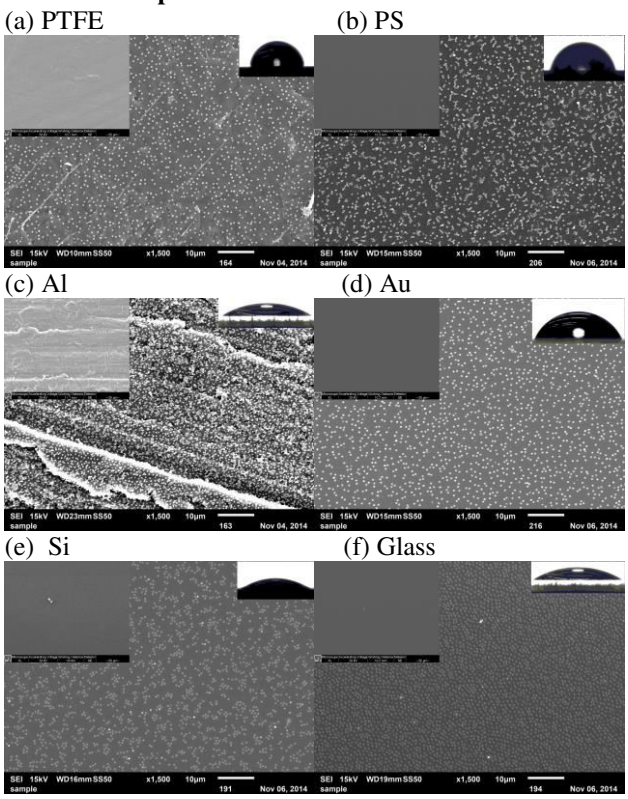

In order to investigate the universality of this method, microgels composed of various functionalities were used to coat surfaces. We investigated unmodified pNIPAm-based microgels; microgels functionalized with acrylic acid (MG-AAC) that are negatively charged at pH 8.5; microgels functionalized with pyridine (MG-Py) that are neutral at pH 8.5; and microgels functionalized with a quaternary ammonium group (MG-QN) that are positively charged at all pH's. The microgel syntheses are detailed and shown schematically in Figure S4. The results showed that all of the microgels yielded films after exposure to dopamine, using the same conditions as above (Figure S5). The resultant microgel-based films can subsequently be used for various applications. For example, positively charged microgels have been used as a nucleic acid carrier[57,58]; charged drugs, such as doxorubicin, can be incorporated into and released from charged microgels; pyridine can coordinate metal ions, which allows for possible nanoparticle formation in the microgels and thin films.

2.2 Applications of microgel films

Relatedly, we wanted to demonstrate that this surface coating approach could be used for a variety of applications. For example, we show here that films can be generated from microgels doped with: 1) crystal violet (CV); 2) pyridinium hemicyanine (PHC); and 3) silver nanoparticles (Ag NPs). As we describe below, the resulting films can be used as fluorescent surfaces/light emitters, for biological applications, as biomaterials, and for sensing. These are described in detail below.

2.2.1 Microgel films for fluorescent surfaces/light emitters

First, we show that fluorescent/light emitting thin films could be generated. These films were constructed from CV-modified microgels; CV was incorporated into the microgels via the electrostatic interaction between the microgel COO^- groups and the positively charged CV at pH 8.0. This is detailed schematically in SI. Briefly, CV and microgels (1:1 mol:mol) were mixed in H_2O at pH 8.0, and after 5 min the blue/purple CV solution became colorless. Correspondingly, the microgels clearly transitioned from colorless to blue (Figure S6a). UV-vis results revealed that 98.2% of CV was incorporated into microgels (Figure S6b). Furthermore, UV-vis of the CV-modified microgels showed a characteristic adsorption peak at 590 nm, indicating CV was successfully incorporated into microgels. The content of CV was controlled by adjusting content of carboxylic acid in microgels. Next, films composed of the CV-modified microgels were generated on glass slides, and their fluorescence investigated via excitation at 405 nm while monitoring the emission at 500 nm. As can be seen from the fluorescence microscopy images in Figure 3 and S7, the resulting films exhibit strong fluorescence. We also showed that the emission intensity from the microgel films increased with increasing of CV content in the microgel, (Figure S7) demonstrating that the emission intensity can be tuned by adjusting the amount of CV in microgels.

Figure 3. (a) Fluorescence microscopy image of thin films composed of CV-modified microgels (excited at 405 nm) and (b) PHC-modified microgels (excited at 920 nm) -- scale bar is 4 μm in both images. Insets show that the fluorescence intensity from the films increases with fluorophore content in the microgels.

(a) (b)

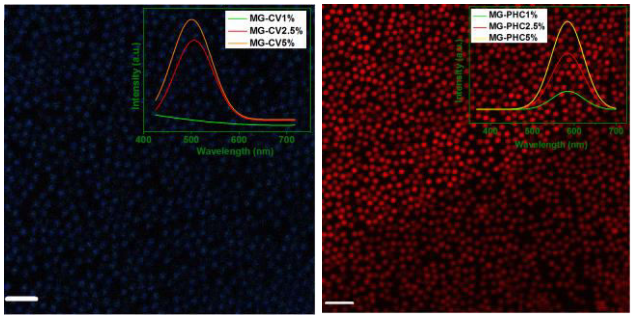

Next, we showed that microgels composed of a two-photon excited fluorophore (TPF) could be fabricated, and thin films constructed. TPFs are capable of absorbing two photons of identical frequency (low frequency, relative to a single photon excited fluorophore) to excite a molecule from the ground state to an excited electronic state. The ability to excite molecules with two low energy photons increases photostability of materials. One shortcoming that has limited the use of TPF in materials is quenching induced by aggregation, particularly in the solid state. Recently, the Chen and Qian groups showed that cationic PHC could be incorporated into a metal-organic framework (MOF) to minimize this phenomenon.[59] Relatedly, microgels also have a porous structure (akin to MOFs), in which PHC can be incorporated; we hypothesize that incorporating PHC into the microgel network will also help prevent this quenching effect. Initially, PHC was synthesized, as shown in experimental section, and incorporated into microgels via electrostatic interaction using the same method with CV loading process. Then, microgel films were prepared using the PHC loading microgels. An image and emission spectra of PHC microgel films are shown in Figure 3b. As can be seen, the film exhibited strong fluorescence at 590 nm after excitation at 920 nm, as shown in Figure 3b. Like CV loaded microgel films, the fluorescence is attributed to PHC-modified microgels and their emission intensity can be controlled by adjusting the PHC content in the microgels.

2.2.2 Microgel films for antibacterial coating

In a subsequent experiment, we showed that antibacterial films could be generated using microgel modified with silver nanoparticles (Ag NPs). As is well known, bacteria can adhere to solid surfaces, where they can form colonies and subsequent biofilms, which can cause material damage and pathogenic infections. Therefore, the prevention of biofilm formation is of utmost importance, and has been of recent interest to biomaterials researchers. Ag NPs were shown to exhibit antimicrobial activity exhibiting strong cytotoxicity toward a broad range of microorganisms, while exhibiting low known toxicity in humans. Ag's potency comes from its oligodynamic effect, i.e., Ag can result in a bacteriostatic (growth inhibition), and bactericidal (antibacterial) effect. In the current work, Ag NPs were incorporated into microgels using an in situ generation method. First, microgels were exposed to Ag^+ at pH = 8, which rendered them negatively charged (COO^-) and able to complex Ag^+. Ag^+ was subsequently reduced by exposure to $NaBH_4$ to obtain Ag nanoparticles. The process was monitored by XPS, and the results are shown in Figure S8. Two Ag 3d3/2 and 3d5/2 characteristic peaks were observed at 367.9 and 373.9 eV, respectively for MG-Ag^+. These regions are very sensitive to the chemical environment surrounding the Ag and can provide important information to distinguish between Ag^+ and Ag^0. After reduction by $NaBH_4$, these peaks shifted to 365.5 and 371.5 eV, which are characteristic of 3d3/2 and 3d5/2 of Ag NPs, respectively. The result indicated that Ag^+ was completely reduced to Ag NPs. For comparison, MG without AAC was also tested, and no Ag characteristic peak was observed. The content of Ag NPs was tested by thermogravimetric analysis (TGA), and the result is shown in Figure S9. These data revealed that the microgels were 26 % (weight percent) Ag NPs. In order to investigate this system's practical application as an antibacterial coating, a MG-Ag^0 film was prepared on glass slide. A microscope and TEM image of a MG-Ag^0 film is shown in Figure 4. Gram-negative Escherichia coli (*E. coli*) and gram-positive Bacillus subtilis (*B. subtilis*) were used as model bacteria in these tests. For comparison, a glass substrate coated with a microgel film without Ag^0 was also tested. A suspension of bacteria (1×10^6 CFU mL^{-1}) was sprayed onto the respective MG-Ag^0 and MG-AAC films modified glass slides using a commercial chromatography sprayer (VWR Scientific) (spray rate of 5 mL/min). After air-drying, the slides were placed in Petri dishes, and then growth agar (Luria-Bertani agar for *E. coli* and nutrient agar for *B. Subtilis*) was added. The Petri dishes were sealed and incubated for 20 h at 37 °C. Then, the slides were removed, washed with H_2O to remove agar and bacteria not directly attached to the substrates. Figure 4 shows representative microscope images of MG-AAC and MG-Ag^0 films after exposure to *E. coli* and *B. subtilis*. A high *E. coli* and *B. subtilis* density was observed on surfaces modified with microgels lacking Ag^0, while no bacteria were observed on the surface of MG-Ag^0 film; this clearly shows the excellent antibacterial properties of the MG-Ag^0 film.

Figure 4 Bacteria growth on microgel films. (a): *E. coli* on MG-AAC film; (b): *E. coli* on MG-Ag^0 film; (c): *B. subtilis* on MG-AAC film; and (d): *B. subtilis* on MG-Ag^0 film. Insets are TEM images of a single representative microgel-MG-AAC in (a), MG-Ag^0 in (b). The scale bar in all images is 4 µm.

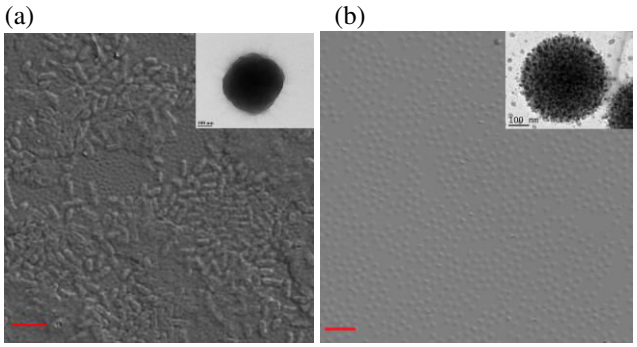

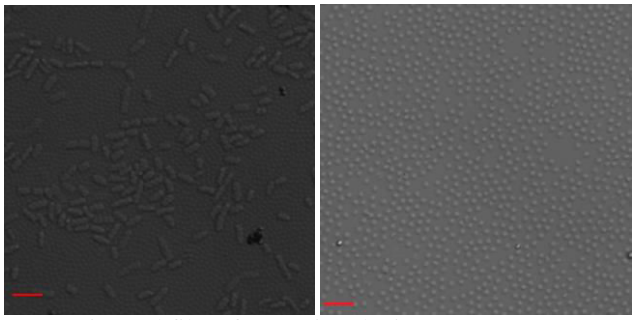

2.2.3 Microgel films for sensing device

Finally, we show that the microgel-based thin films can be used for sensing applications. To show this, an optical device (etalon) was constructed by thermally evaporating a 15 nm Au layer on a MG-AAC film formed on an Al substrate. The device structure is shown schematically in Figure 5a, while the complete fabrication details have been previously reported by our group.[59,60] When light impinges on the device, it is able to enter the microgel-based cavity and resonate, leading to constructive/destructive interference, which results in color and a multipeak reflectance spectrum.[61-64] The spectrum that results can be described by equation (1) for the interference of light in an optical cavity:

$$m\lambda = 2 n d \cos\theta \qquad (1)$$

where λ is the wavelength maximum for reflected light, m is the peak order, n is the refractive index of the dielectric, d is the spacing between the mirrors, and θ is the angle of incidence. λ is directly proportional to the distance between the Au and Al layers (d), which is directly related to the thickness of the film between the two layers, as shown in Figure 5b. Therefore, any stimuli that can trigger a microgel size change will lead to a shift in the position of the peaks in the reflectance spectrum.

Figure 5. (a, b) Schematic depiction of optical device. In (a), the layers are a - substrate; b, d- Au layers; and c- a microgel layer. (c) Reflectance spectra of the sensing device at pH = 3 and 6. (d) Peak position as a function of pH at 30 °C. Each point is the average from three repeat experiments with a single device, while the error bars indicate standard deviation.

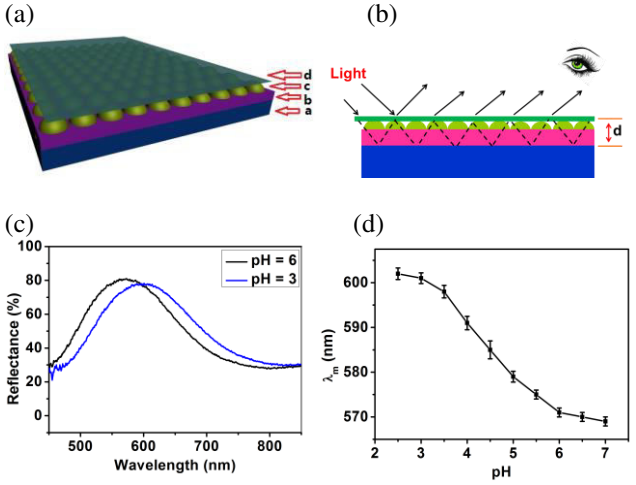

Figure 5c shows representative reflectance spectra for a device at pH = 3 and 6. As can be seen, as the pH decreases (from pH = 6 to pH = 3) the position of the reflectance peak red shifts ~30 nm (Figure 5d). We propose that this is observed due to the presence of free amines within the microgels due to dopamine penetrating into the microgel pores. The pKa values of R–COOH and R'–NH_2 are ~4.25 and 10.0 respectively. At pH = 6, positively charged polydopamine (R'–NH_3^+) is capable of crosslinking the negatively charged MG-AAC microgels (R-COO^-), resulting in microgel collapse. When the solution pH is decreased to 3, the microgel's negative charges are neutralized, breaking the electrostatic bond with the protonated dopamine groups. This breaks the electrostatic crosslinks holding the microgels in a collapsed state, resulting in microgel swelling. This yields an increase in the distance between the gold layer and Al, and a concomitant red shift of the reflectance peaks, according to equation (1). A similar approach can be used for biosensing applications, and will be the topic of future investigations.

CONCLUSIONS

In summary, a variety of microgel films were prepared on various materials (metals, non-metals, and polymers). We showed that the density of the microgels in the films was related to the hydrophilicity of the starting material. We showed that microgels with 4 different chemistries -- modified to be positively charged, negatively charged, neutral and modified with pyridine -- could be used to fabricate films and they can be used for various applications. For example, we showed that surfaces could be rendered fluorescent, antibacterial, and optically active via this very simple and straightforward protocol. The simplicity and apparent universality of this approach makes it a very powerful surface modification strategy, which can find many future applications in many areas only limited by imagination.

EXPERIMENT

Synthesis of pyridinium hemicyanine

4-Picoline (4.65 g, 0.05 mol) was dissolved in tetrahydrofuran (100 mL) and stirred vigorously while methyl iodide (28.35 g, 0.20 mmol, 1.25 mL) was added. The resultant mixture was refluxed for 6 h. The solid was separated by filtration. Yield: 85%. ^{1}H NMR (DMSO-d_6, δ ppm.): 8.8 (d, 2H), 7.9 (d, 2H), 4.2 (s, 3H); MS (M+H): 235.99.

To a solution of 4-(N, N-dimethylamino)benzaldehyde (14.95 g, 100 mmol) and 1,4-dimethylpyridinium iodide (23.10 g, 98 mmol) in ethanol (250 mL) was added piperidine (2.00 mL). The yellow solution was refluxed for 1 day and then cooled to room temperature. The resultant precipitate was collected and recrystallized from methanol to yield red needle-like crystals of PHC. Yield: 78%. ^{1}H NMR (DMSO-d_6, δ ppm.): 8.67 (d, 2 H), 8.04 (d, 2 H), 7.90 (d, 1 H), 7.59 (d, 2 H), 7.17 (d, 1 H), 6.78 (d, 2 H), 4.17 (s, 3 H), 3.02 (s, 6 H). MS (M+H): 367.06.

Preparation of MG-Ag^0

0.1 g MG-AAC was soaked in 10 mL aqueous $AgNO_3$ (0.1 mol L^{-1}) for 24 h to allow the Ag ion to be absorbed into the microgel via ion exchange, and then washed thoroughly using multiple centrifugation/water resuspensi-

on cycles to remove any excess $AgNO_3$. A 10-fold excess of aqueous $NaBH_4$ (relative to the Ag ion) was added to the microgels with vigorous stirring, then the mixture was kept at RT for 12 h. The resultant MG-Ag^0 was collected by centrifugation, resuspended in water, which was repeated 6 times, and freeze-dried at room temperature for 24 h.

Preparation of microgel films

0. 2 g Dopamine and 0.02 g microgels were dissolved in 20 mL DI water. The pH of the solution was adjusted to 8.5, and the substrates were immersed into the solution. The pH-induced oxidation causes the solution to change color from colorless to dark brown. After 24 h, the coated surfaces were rinsed with DI water and dried with N_2 gas before storage.

Antimicrobial Activity Assay

Colony forming units (CFU) of *E. coli* and *B. subtilis* was determined (using BioMate 3S Spectrophotometer) from the measured absorbance at 600 nm using previously established standard calibration curves. A suspension of E. coli and B. subtilis (1.5×10^6) was then sprayed onto microgel films attached to glass slides in a fume hood using a commercial chromatography sprayer (VWR Scientific) (spray rate of 10 mL/min). After drying for 10 min in air, the slide was placed in a Petri dish, and then growth agar (Luria-Bertani agar for *E. coli* and nutrient agar for *B. Subtilis*, was autoclaved, and cooled to 37 °C) was added. The Petri dish was closed, sealed, and incubated at 37 °C overnight. The samples were then washed using DI water to remove the dead and unattached bacteria and subsequently analyzed.

ACKNOWLEDGEMENTS

MJS acknowledges funding from the University of Alberta (the Department of Chemistry and the Faculty of Science), the Natural Sciences and Engineering Research Council of Canada (NSERC), the Canada Foundation for Innovation (CFI), the Alberta Advanced Education & Technology Small Equipment Grants Program (AET/SEGP) and Grand Challenges Canada.

ASSOCIATED CONTENT

Supporting Information Available: Characterization methods, microgel synthesis scheme, dynamic light scattering measurements of microgel diameter, reflectance spectra for etalon devices, SEM/TEM images of samples, optical microscope images, and cell images are available as Supporting Information. This material is available free of charge via the Internet at http://pubs.acs.org."

REFERENCES:

(1) Yu, H.; Qiu, X.; Nunes, S. P.; Peinemann, K.-V. Self-assembled Isoporous Block Copolymer Membranes with Tuned Pore Sizes. *Angew. Chem. Int. Ed.* **2014**, *53*, 10236-10240.

(2) Wen, L.; Tian, Y.; Jiang, L. Bioinspired Super-Wettability from Fundamental Research to Practical Applications. *Angew. Chem. Int. Ed.* **2015**, *54*, 3387-3399.

(3) Adera, S.; Raj, R.; Enright, R.; Wang, E. N. Non-Wetting Droplets on Hot Superhydrophilic Surfaces. *Nat. Commun.* **2013**, *4*, 2518-2525.

(4) Kango, S.; Kalia, S.; Celli, A.; Njuguna, J.; Habibi, Y.; Kumar, R. Surface Modification of Inorganic Nanoparticles for Development of Organic-Inorganic Nanocomposites-A Review. *Prog. Polym. Sci.* **2013**, *38*, 1232-1261.

(5) Tauhardt, L.; Kempe, K.; Gottschaldt, M.; Schubert, U. S. Poly(2-oxazoline) Functionalized Surfaces: from Modification to Application. *Chem. Soc. Rev.* **2013**, *42*, 7998-8011.

(6) Liu, H.; Li, Y.; Sun, K.; Fan, J.; Zhang, P.; Meng, J.; Wang, S.; Jiang, L. Dual-Responsive Surfaces Modified with Phenylboronic Acid-Containing Polymer Brush to Reversibly Capture and Release Cancer Cells. *J. Am. Chem. Soc.* **2013**, *135*, 7603-7609.

(7) Tian, Y.; Jiang, L. Wetting: Intrinsically Robust Hydrophobicity. *Nat. Mater.* **2013**, *12*, 291-292.

(8) Kim, B. J.; Park, T.; Moon, H. C.; Park, S. Y.; Hong, D.; Ko, E. H.; Kim, J. Y.; Hong, J. W.; Han, S. W.; Kim, Y. G.; Choi, I. S. Cytoprotective Alginate/Polydopamine Core/Shell Microcapsules in Microbial Encapsulation. *Angew. Chem. Int. Ed.* **2014**, *53*, 14443-14446.

(9) Pang, S. H.; Schoenbaum, C. A.; Schwartz, D. K.; Medlin, J. W. Directing Reaction Pathways by Catalyst Active-site Selection Using Self-assembled Monolayers. *Nat. Commun.* **2013**, *4*, 2448-2454.

(10) Sayed, S. Y.; Bayat, A.; Kondratenko, M.; Leroux, Y.; Hapiot, P.; McCreery, R. L. Bilayer Molecular Electronics: All-carbon Electronic Junctions Containing Molecular Bilayers Made with "Click" Chemistry. *J. Am. Chem. Soc.* **2013**, *135*, 12972-12975.

(11) Zaba, T.; Noworolska, A.; Bowers, C. M.; Breiten, B.; Whitesides, G. M.; Cyganik, P. Formation of Highly Ordered Self-assembled Monolayers of Alkynes on Au(111) Substrate. *J. Am. Chem. Soc.* **2014**, *136*, 11918-11921.

(12) Decher, G. Fuzzy Nanoassemblies: Toward Layered Polymeric Multicomposites. *Science* **1997**, *277*, 1232-1237.

(13) Xiao, M.; Huang, F.; Huang, W.; Dkhissi, Y.; Zhu, Y.; Etheridge, J.; Gray-Weale, A.; Bach, U.; Cheng, Y.-B.; Spiccia, L. A Fast Deposition-Crystallization Procedure for Highly Efficient Lead Iodide Perovskite Thin-Film Solar Cells. *Angew. Chem. Int. Ed.* **2014**, *53*, 10056-10061.

(14) Yan, J.; Li, B.; Yu, B.; Huck, W. T. S.; Liu, W.; Zhou, F. Controlled Polymer-Brush Growth from Microliter Volumes Using Sacrificial-Anode Atom-Transfer Radical Polymerization. *Angew. Chem. Int. Ed.* **2013**, *52*, 9125-9129.

(15) Baghbanzadeh, M.; Simeone, F. C.; Bowers, C. M.; Liao, K.-C.; Thuo, M.; Baghbanzadeh, M.; Miller, M. S.; Carmichael, T. B.; Whitesides, G. M. Odd–Even Effects in Charge Transport Across n-Alkanethiolate-Based SAMs. *J. Am. Chem. Soc.* **2014**, *136*, 16919-16925.

(16) Zaba, T.; Noworolska, A.; Bowers, C. M.; Breiten, B.; Whitesides, G. M.; Cyganik, P. Formation of Highly Ordered Self-Assembled Monolayers of Alkynes on Au (111) Substrate. *J. Am. Chem. Soc.* **2014**, *136*, 11918-11921.

(17) Love, J. C.; Estroff, L. A.; Kriebel, J. K.; Nuzzo, R. G.; Whitesides, G. M. Self-Assembled Monolayers of Thiolates on Metals as A Form of Nanotechnology. *Chem. Rev.* **2005**, *105*, 1103-1170.

(18) Xue, Y.; Li, X.; Li, H.; Zhang, W. Quantifying Thiol-Gold Interactions towards the Efficient Strength Control. *Nat. Commun.* **2014**, *5*, 4348-4357.

(19) Yu, Z.; Pan, Y.; Shen, Y.; Wang, Z.; Ong, Z.-Y.; Xu, T.; Xin, R.; Pan, L.; Wang, B.; Sun, L.; Wang, J.; Zhang,

G.; Zhang, Y. W.; Shi, Y.; Wang, X. Towards Intrinsic Charge Transport in Monolayer Molybdenum Disulfide By Defect and Interface Engineering. *Nat. Commun.* **2014**, *5*, 5290-5297.
(20) van Delden, R. A.; ter Wiel, M. K. J.; Pollard, M. M.; Vicario, J.; Koumura, N.; Feringa, B. L. Unidirectional Molecular Motor on A Gold Surface. *Nature* **2005**, *437*, 1337-1340.
(21) Gautier, C.; Buergi, T. Chiral N-isobutyryl-cysteine Protected Gold Nanoparticles: Preparation, Size Selection, and Optical Activity in the UV-vis and Infrared. *J. Am. Chem. Soc.* **2006**, *128*, 11079-11087.
(22) Lv, Z.; Wang, J.; Chen, G. Self-assembled Human IgG Monolayers on Mixed Thiols Modified Gold Surfaces. *Asian J. Chem.* **2013**, *25*, 3237-3243.
(23) An, Q.; Brinkmann, J.; Huskens, J.; Krabbenborg, S.; de Boer, J.; Jonkheijm, P. Supramolecular System for the Electrochemically Controlled Release of Cells. *Angew. Chem. Int. Ed.* **2012**, *51*, 12233-12237.
(24) Srisombat, L.; Jamison, A. C.; Lee, T. R. Stability: A Key Issue for Self-assembled Monolayers on Gold as Thin-film Coatings and Nanoparticle Protectants. *Colloids Surf. A* **2011**, *390*, 1-19.
(25) Schlenoff, J. B.; Li, M.; Ly, H. Stability and Self-exchange in Alkanethiol Monolayers. *J. Am. Chem. Soc.* **1995**, *117*, 12528-12536.
(26) Karahan, H. E.; Eyüboğlu, L.; Kıyılar, D.; Demirel, A. L. pH-stability and pH-Annealing of H-bonded Multilayer Films Prepared by Layer-by-Layer Spin-assembly. *Eur. Polym. J.* **2014**, *56*, 159-167.
(27) Borges, J.; Mano, J. F. Molecular Interactions Driving the Layer-by-Layer Assembly of Multilayers. *Chem. Rev.* **2014**, *114*, 8883-8942.
(28) Singh, A.; Corvelli, M.; Unterman, S. A.; Wepasnick, K. A.; McDonnell, P.; Elisseeff, J. H. Enhanced Lubrication on Tissue and Biomaterial Surfaces Through Peptide-Mediated Binding of Hyaluronic Acid. *Nat. Mater.* **2014**, *3*, 988-995.
(29) Rana, D.; Matsuura, T. Surface Modifications for Antifouling Membranes. *Chem. Rev.* **2010**, *110*, 2448-2471.
(30) Lee, H.; Dellatore, S. M.; Miller, W. M.; Messersmith, P. B. Mussel-Inspired Surface Chemistry for Multifunctional Coatings. *Science* **2007**, *318*, 426-430.
(31) Wei, Q.; Achazi, K.; Liebe, H.; Schulz, A.; Noeske, P. L. M.; Grunwald, I.; Haag, R. Mussel- Inspired Dendritic Polymers as Universal Multifunctional Coatings. *Angew. Chem. Int. Ed.* **2014**, *53*, 11650-11655.
(32) Ham, H. O.; Liu, Z.; Lau, K.; Lee, H.; Messersmith, P. B. Facile DNA Immobilization on Surfaces Through A Catecholamine Polymer. *Angew. Chem. Int. Ed.* **2011**, *123*, 758-762.
(33) Ryou, M. H.; Kim, J.; Lee, I.; Kim, S.; Jeong, Y. K.; Hong, S.; Ryu, J. H.; Kim, T. S.; Park, J. K.; Lee, H. Mussel- Inspired Adhesive Binders for High- Performance Silicon Nanoparticle Anodes in Lithium- Ion Batteries. *Adv. Mater.* **2013**, *25*, 1571-1576.
(34) Ham, H. O.; Liu, Z.; Lau, K. H. A.; Lee, H.; Messersmith, P. B. Facile DNA Immobilization on Surfaces Through A Catecholamine Polymer. *Angew. Chem. Int. Ed.* **2011**, *123*, 758-762.
(35) Sileika, T. S.; Barrett, D. G.; Zhang, R.; Lau, K. H. A.; Messersmith, P. B. Colorless Multifunctional Coatings Inspired by Polyphenols Found in Tea, Chocolate, and Wine. *Angew. Chem. Int. Ed.* **2013**, *52*, 10766-10770.
(36) García- Fernández, L.; Cui, J.; Serrano, C.; Shafiq, Z.; Gropeanu, R. A.; Miguel, V. S.; Ramos, J. I.; Wang, M.; Auernhammer, G. K.; Ritz, S. Antibacterial Strategies from the Sea: Polymer- Bound Cl- Catechols for Prevention of Biofilm Formation. *Adv. Mater.* **2013**, *25*, 529-533.
(37) Fullenkamp, D. E.; Rivera, J. G.; Gong, Y.-k.; Lau, K. H. A.; He, L.; Varshney, R.; Messersmith, P. B. Mussel-Inspired Silver-Releasing Antibacterial Hydrogels. *Biomaterials* **2012**, *33*, 3783-3791.
(38) Zhou, J. J.; Duan, B.; Fang, Z.; Song, J. B.; Wang, C. X.; Messersmith, P. B.; Duan, H. W. Interfacial Assembly of Mussel-Inspired Au@Ag@ Polydopamine Core-Shell Nanoparticles for Recyclable Nanocatalysts. *Adv. Mater.* **2014**, *26*, 701-705.
(39) Ham, H. O.; Park, S. H.; Kurutz, J. W.; Szleifer, I. G.; Messersmith, P. B. Antifouling Glycocalyx-Mimetic Peptoids. *J. Am. Chem. Soc.* **2013**, *135*, 13015-13022.
(40) Barrett, D. G.; Bushnell, G. G.; Messersmith, P. B. Mechanically Robust, Negative-Swelling, Mussel-Inspired Tissue Adhesives. *Adv. Healthc. Mater.* **2013**, *2*, 745-755.
(41) Kang, S. M.; Hwang, N. S.; Yeom, J.; Park, S. Y.; Messersmith, P. B.; Choi, I. S.; Langer, R.; Anderson, D. G.; Lee, H. One-Step Multipurpose Surface Functionalization by Adhesive Catecholamine. *Adv. Funct. Mater.* **2012**, *22*, 2949-2955.
(42) Yu, J.; Kan, Y.; Rapp, M.; Danner, E.; Wei, W.; Das, S.; Miller, D. R.; Chen, Y.; Waite, J. H.; Israelachvili, J. N. Adaptive Hydrophobic and Hydrophilic Interactions of Mussel Foot Proteins with Organic Thin Films. *Proc. Natl. Acad. Sci. U. S. A.* **2013**, *110*, 15680-15685;
(43) Ahn, B. K.; Lee, D. W.; Israelachvili, J. N.; Waite, J. H. Surface-Initiated Self-Healing of Polymers in Aqueous Media. *Nat. Mater.* **2014**, *13*, 867-872.
(44) Wei, W.; Yu, J.; Broomell, C.; Israelachvili, J. N.; Waite, J. H. Hydrophobic Enhancement of Dopa-Mediated Adhesion in A Mussel Foot Protein. *J. Am. Chem. Soc.* **2012**, *135*, 377-383.
(45) Wattanakit, C.; Saint Côme, Y. B.; Lapeyre, V.; Bopp, P. A.; Heim, M.; Yadnum, S.; Nokbin, S.; Warakulwit, C.; Limtrakul, J.; Kuhn, A. Enantioselective Recognition at Mesoporous Chiral Metal Surfaces. *Nat. Commun.* **2014**, *5*, 3325-3333.
(46) Park, J.; Brust, T. F.; Lee, H. J.; Lee, S. C.; Watts, V. J.; Yeo, Y. Polydopamine-Based Simple and Versatile Surface Modification of Polymeric Nano Drug Carriers. *ACS Nano* **2014**, *8*, 3347-3356.
(47) Zhou, W.; Xiao, X.; Cai, M.; Yang, L. Polydopamine-Coated, Nitrogen-Doped, Hollow Carbon–Sulfur Double-Layered Core–Shell Structure for Improving Lithium–Sulfur Batteries. *Nano Lett.* **2014**, *14*, 5250-5256.
(48) Yu, X.; Fan, H.; Wang, L.; Jin, Z. Formation of Polydopamine Nanofibers with the Aid of Folic Acid. *Angew. Chem. Int. Ed.* **2014**, *53*, 12600-12604.
(49) Tang, J.; Liu, J.; Li, C.; Li, Y.; Tade, M. O.; Dai, S.; Yamauchi, Y. Synthesis of Nitrogen- Doped Mesoporous Carbon Spheres with Extra- Large Pores Through As-

sembly of Diblock Copolymer Micelles. *Angew. Chem. Int. Ed.* **2015**, *54*, 588-593.
(50) Tang, W.; Policastro, G. M.; Hua, G.; Guo, K.; Zhou, J.; Wesdemiotis, C.; Doll, G. L.; Becker, M. L. Bioactive Surface Modification of Metal Oxides via Catechol-Bearing Modular Peptides: Multivalent-Binding, Surface Retention, and Peptide Bioactivity. *J. Am. Chem. Soc.* **2014**, *136*, 16357-16367.
(51) Wei, Q.; Becherer, T.; Noeske, P. L. M.; Grunwald, I.; Haag, R. A Universal Approach to Crosslinked Hierarchical Polymer Multilayers as Stable and Highly Effective Antifouling Coatings. *Adv. Mater.* **2014**, *26*, 2688-2693.
(52) Geisel, K.; Isa, L.; Richtering, W. The Compressibility of pH-Sensitive Microgels at the Oil–Water Interface: Higher Charge Leads to Less Repulsion. *Angew. Chem. Int. Ed.* **2014**, *53*, 5005-5009.
(53) Hendrickson, G. R.; Smith, M. H.; South, A. B.; Lyon, L. A. Design of Multiresponsive Hydrogel Particles and Assemblies. *Adv. Funct. Mater.* **2010**, *20*, 1697-1712.
(54) Lyon, L. A.; Meng, Z.; Singh, N.; Sorrell, C. D.; St. John, A. Thermoresponsive Microgel-Based Materials. *Chem. Soc. Rev.* **2009**, *38*, 865-874.
(55) Kim, J.; Serpe, M. J.; Lyon, L. A. Photoswitchable Microlens Arrays. *Angew. Chem. Int. Ed.* **2005**, *117*, 1357-1360.
(56) Della Vecchia, N. F.; Avolio, R.; Alfè, M.; Errico, M. E.; Napolitano, A.; d'Ischia, M. Building-Block Diversity in Polydopamine Underpins a Multifunctional Eumelanin-Type Platform Tunable Through A Quinone Control Point. *Adv. Funct. Mater.* **2013**, *23*, 1331-1340;
(57) Chen, K.; Xu, J.; Luft, J. C.; Tian, S.; Raval, J. S.; DeSimone, J. M. Design of Asymmetric Particles Containing A Charged Interior and A Neutral Surface Charge: Comparative Study on In Vivo Circulation of Polyelectrolyte Microgels. *J. Am. Chem. Soc.* **2014**, *136*, 9947-9952.
(66) Shim, M. S.; Xia, Y. A Reactive Oxygen Species (ROS)-Responsive Polymer for Safe, Efficient, and Targeted Gene Delivery in Cancer Cells. *Angew. Chem. Int. Ed.* **2013**, *52*, 7064-7067.
(58) Yu, J.; Cui, Y.; Xu, H.; Yang, Y.; Wang, Z.; Chen, B.; Qian, G. Confinement of Pyridinium Hemicyanine Dye within An anionic Metal-Organic Framework For Two-Photon-Pumped Lasing. *Nat. Commun.* **2013**, *4*, 2719-2726.
(59) Sorrell, C. D.; Serpe M. J. Reflection Order Selectivity of Color- Tunable Poly (N- Isopropylacrylamide) Microgel Based Etalons. *Adv. Mater.* **2011**, *23*, 4088-4092.
(60) Sorrell, C. D.; Carter, M. C.; Serpe M. J. Color Tunable Poly (N- Isopropylacrylamide)- co- Acrylic Acid Microgel–Au Hybrid Assemblies. *Adv. Funct. Mater.* **2011**, *21*, 425-433.
(61) Zhang, Q. M.; Xu, W.; Serpe, M. J. Optical Devices Constructed from Multiresponsive Microgels. *Angew. Chem. Int. Ed.* **2014**, *53*, 4827-4831.
(62) Zhang, Q. M.; Li, X.; Islam, M. R.; Wei, M.; Serpe, M. J. Light Switchable Optical Materials from Azobenzene Crosslinked Poly (N-Isopropylacrylamide)-Based Microgels. *J. Mater. Chem. C* **2014**, *2*, 6961-6965.
(63) Zhang, Q. M.; Ahiabu, A.; Gao, Y.; Serpe, M. J. CO2-Switchable Poly (N-Isopropylacrylamide) Microgel-Based Etalons. *J. Mater. Chem. C* **2015**, *3*, 495-498.
(64) Zhang, Q. M.; Berg, D.; Mugo, S. M.; Serpe, M. J. Lipase-Modified pH-Responsive Microgel-Based Optical Device for Triglyceride Sensing. *Chem. Commun.* **2015**, *51*, 9726-9728.

A versatile surface modification method: A versatile surface modification technique was developed to yield microgel-based thin films on a variety of substrates, e.g., metals, non-metals, and polymers. The resulting films can be used as fluorescent surfaces/light emitters, for biological applications, as biomaterials, and for sensing.